Effects of Spinning and Drawing Conditions on the Crimp Contraction of Side-by-Side Poly(trimethylene terephthalate) Bicomponent Fibers

Tae Hwan Oh

Huvis R&D Center, 1690-1, Shinil Dong, Daedeok Ku, Daejeon, South Korea

Received 27 September 2005; accepted 23 December 2005
DOI 10.1002/app.23988
Published online in Wiley InterScience (www.interscience.wiley.com).

ABSTRACT: The crimp properties in the melt-spinning and drawing processes of side-by-side bicomponent fibers with poly(trimethylene terephthalate)s (PTTs) of different viscosities were studied. Two PTTs of different intrinsic viscosities (1.02 and 0.92) were selected to make latent crimp yarn. The spinning and drawing conditions were changed to investigate the relation between the process conditions and crimp contraction. An orthogonal array was used to rule out the weak variables. The draw ratio, heat-set temperature, and portion of high-viscosity PTT were selected as variables having an effect on the crimp contraction. An analysis of the effects of the spinning and drawing conditions on the crimp contraction showed that the draw ratio was the most critical variable. Increasing the draw ratio caused a difference in the shrinkage between the two parts of PTT and caused the self-crimping of the bicomponent fibers. Although changing the heat-set temperature and the portion of high-viscosity PTT did not produce a dimensional change, the crimp contraction varied with those variables. As the heat-set temperature and the high-viscosity portion increased, the crimp contraction increased. © 2006 Wiley Periodicals, Inc. J Appl Polym Sci 102: 1322–1327, 2006

Key words: fibers; orientation; polyesters

INTRODUCTION

Melt spinning is a continuous deformation process and the most widely used method for manufacturing commercial synthetic fibers. It has been developed progressively for manufacturing new fibers with special functions.[1–4] In particular, new fibers[5] have superior function and additional special applications in comparison with natural fibers. Therefore, new fibers possess very wide applicability for various textile products such as clothing, furnishings, and technical textiles. Bicomponent spinning technology has been used to make new fibers. There are common bicomponent fibers such as sea–island, split, sheath–core, and side-by-side types. Side-by-side bicomponent fibers were developed to imitate the crimp properties of wool.[6] The self-crimping properties of wool result from its unique structure, which is created by the ortho-cortex and the para-cortex adhering to each other. The crimp of woolen yarns gives high bulkiness, warm touch, and stretch. Timoshenko[7] used a bimetallic theory to explain the self-crimping behavior. Brown and Onions[8] applied Timoshenko's theory to fibers. Brand and Becker[9] developed a more general theory: the crimp curvature is proportional to the differential length change and inversely proportional to the fiber thickness. Gupta and George[10] revealed the relation between the crimp curvature and the deformation of bicomponent fibers. Fitzgerald and Knudsen[11] formulated equations to explain the relation between the fiber curvature, differential shrinkage, fiber thickness, and cross-sectional component distribution.

Poly(trimethylene terephthalate) (PTT), a newly commercialized polyester, has been watched from the end of the 1990s because of the commercial production of its raw material, 1,3-propanediol. Studies of PTT for fibers, films, and engineering plastics have increased.[12,13] Studies of PTT for fibers have been concentrated on the structure–property relationship of PTT homofibers.[14,15] There is still a lack of studies on PTT bicomponent fibers.

In this work, changes in the physical properties, with a particular focus on crimp contraction in the bicomponent melt-spinning and drawing process of PTT, were studied, and the effect of the process conditions was examined.

EXPERIMENTAL

Materials

The polymers were textile-grade PTTs; the intrinsic viscosities (IVs) were 1.02 for high-viscosity poly(trimethylene terephthalate) (PTT-H) and 0.92 for low-

Correspondence to: T. H. Oh (ohth@huvis.com).

Journal of Applied Polymer Science, Vol. 102, 1322–1327 (2006)

viscosity poly(trimethylene terephthalate) (PTT-L). The number-average molecular weights were 30,100 for PTT-H and 26,967 for PTT-L. The melt viscosity as a function of the shear rate and melting temperature was measured with a piston-type capillary rheometer with a diameter of 0.5 mm and a length-to-diameter ratio of 3. The temperature was monitored at two positions in the barrel and the die section, and the temperature was controlled within ±0.5°C. The diameter of the barrel was 20 mm, and the entrance angle into the capillary was 80°.

Melt spinning and drawing

The side-by-side bicomponent melt-spinning apparatus (MST-II), manufactured by Syntex Co. (UK), and the drawing apparatus (DW-II), manufactured by Ishikawa Seisakusho, Ltd., Japan, were employed to carry out the experiment. As-spun fibers were manufactured with a spinning machine, and then they were drawn. A spinneret plate with 36 bores, a bore diameter of 0.30 mm, and a length-to-diameter ratio of 2 was employed. The spinning and drawing conditions for the screening test are summarized in Table I. An orthogonal array method[16] was used to evaluate the effects of the process variables and to rule out the weak variables. Practical obtainable maximum and minimum values with the spinning and drawing apparatus were selected, and experiments were performed. After the screening test, several different experimental conditions, including the maximum and minimum values used in the screening test, were selected to investigate the effects of the process conditions for each variable in detail (Tables II and III).

Crimp contraction

Under a tension of 45 mg/dtex, a sample of yarn (3333 dtex) was obtained. The sample was heat-treated in hot water (100°C) for 20 min under a load of 0.45 mg/dtex; this did not cause tangling of the yarn, by which a latent crimp was developed. After the load was removed, the sample was cooled for 4 h and dried in the air. One minute after a load of 1.8 mg/dtex was supplied to the dried sample, length L_1 of the yarn was measured. After L_1 was measured, a load of 1.8 plus 180 mg/dtex was applied to the sample, and after 1 min, length L_2 of the yarns was measured. The crimp contraction was calculated according to eq. (1) with the measured L_1 and L_2 values:

$$\text{Crimp contraction } (\%) = [(L_2 - L_1)/L_2] \times 100 \quad (1)$$

TABLE I
Spinning and Drawing Conditions in the Screening Test

Variable	Condition
Spinning temperature (°C)	255, 270
Take-up speed (m/min)	2000, 3000
Drawing speed (m/min)	400, 800
Drawing temperature (°C)	40, 60
Draw ratio	1.2, 1.5
Portion of PTT-H (%)	35, 65
Heat-set temperature (°C)	160, 200
Quench air velocity (m/s)	0, 0.4

TABLE II
Spinning and Drawing Conditions of the Bicomponent Fibers

Draw ratio	Heat-set temperature (°C)	Portion of PTT-H (%)	Linear density of drawn fiber (dtex)/ number of filaments
1.2	180	55	128.9/36
1.3	180	55	119.3/36
1.4	180	55	112.2/36
1.5	180	55	104.1/36
1.4	160	55	112.1/36
1.4	200	55	112.1/36
1.4	180	35	112.0/36
1.4	180	45	112.1/36
1.4	180	65	112.0/36

Spinning temperature = 265°C; take-up speed = 2500 m/min; quench air velocity = 0.3 m/s; drawing speed = 600 m/min; drawing temperature = 55°C.

Birefringence

The retardation of the optical path of the fibers was measured with a Nikon Optical-Pol polarizing microscope (Japan) and was measured by a compensator method. The wavelength was fixed to 546 nm. The birefringence (Δn) was calculated with the following equation:[17]

$$\Delta n = \frac{\Gamma}{d} \quad (2)$$

where Γ is the retardation of the optical path and d is the thickness of the sample.

TABLE III
Spinning and Drawing Conditions of the Homofibers

Draw ratio	Heat-set temperature (°C)	Linear density of the drawn fiber (dtex)/ number of filaments	
		PTT-H	PTT-L
1.2	180	127.9/36	128.1/36
1.3	180	118.6/36	118.4/36
1.4	180	111.2/36	111.0/36
1.5	180	103.7/36	103.4/36
1.4	160	111.4/36	111.1/36
1.4	200	111.3/36	111.3/36

Spinning temperature = 265°C; take-up speed = 2500 m/min; quench air velocity = 0.3 m/s; drawing speed = 600 m/min; drawing temperature = 55°C.

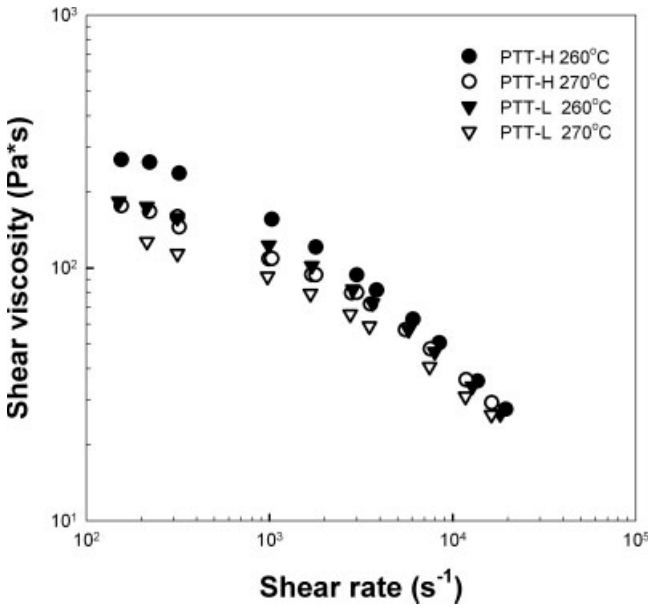

Figure 1 Shear viscosity of PTT-H and PTT-L as a function of the shear rate at different temperatures.

IV and density

After each polymer was sufficiently dissolved in a 1% *ortho*-chlorophenol solution of 120°C, IV was measured in a water bath of 30°C with an Ubbelohde viscometer (Daehan Co., Korea).

The density was measured on small loops of filaments with a density gradient column at 23°C, which contained *n*-heptane and carbon tetrachloride. The volume fraction crystallinity (X_v) was calculated from the measured filament density (ρ) with the following equation:

$$X_v(\%) = \frac{\rho - \rho_a}{\rho_c - \rho_a} \times 100 \quad (3)$$

where ρ_c and ρ_a are the densities of fully crystalline and amorphous polymers, respectively. For PTT, $\rho_c = 1.429$ g/cm^3 and $\rho_a = 1.295$ g/cm^3 were used.[18]

Shrinkage

A sample of a bundle of yarn (3333 dtex) was obtained. After a load of 1.8 mg/dtex was supplied to the sample, which caused no deformation, length L_i of the yarns was measured. The sample was immersed in boiling water for 30 min. After the load was removed, the sample was cooled for 4 h and dried in the air. A load of 1.8 plus 180 mg/dtex was applied to the sample, and after 1 min, length L_f of the yarns was measured. The shrinkage was calculated according to eq. (4) with the measured L_i and L_f values:

$$\text{Shrinkage } (\%) = [(L_i - L_f)/L_i] \times 100 \quad (4)$$

RESULTS AND DISCUSSION

Figure 1 shows the rheological characteristics of PTTs of different IVs. The melt viscosity of PTT shows shear-thinning behavior. The melt viscosity difference at 260°C amounts to 85 Pa s. Figure 2 shows cross-section and side views of the bicomponent fiber. There is curvature [Fig. 2(a)] between PTT-H and PTT-L due to the melt viscosity difference between the two polymers. The cross section of PTT-L shows a crescent shape. Figure 2(b,c) show the side view of drawn fibers and fibers after boiling in the hot water. After the boiling, the latent crimp reveals that the number of curls increases and the size of the crimp decreases.

In the screening test, a response variable was the crimp contraction related to the stretch and recovery properties of the fibers. Figure 3 shows the results of the Pareto chart with a level of significance of 0.1. As shown in the result of the Pareto chart, the statistically meaningful effective variables are the draw ratio, heat-set temperature, and portion of PTT-H. After the screening test, the main variables were investigated.

Effect of the draw ratio

Figure 4 shows the effect of the draw ratio on the crimp contraction. The crimp contraction increases with the draw ratio. This is caused by a shrinkage difference due to a molecular orientation difference between the PTTs of different viscosities that occurs after the extension of side-by-side bicomponent fibers. The crimp contraction increases swiftly in the

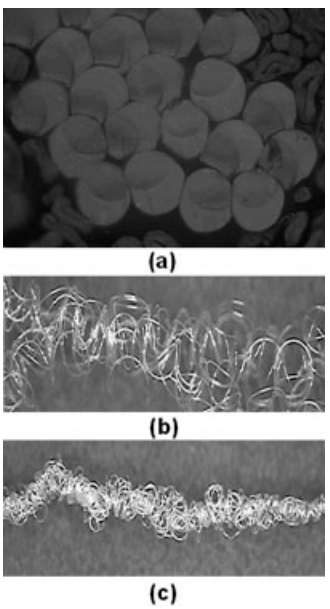

Figure 2 Cross-section and side views of the bicomponent fiber: (a) cross-section view (400×), (b) side view before boiling (40×), and (c) side view after boiling (40×).

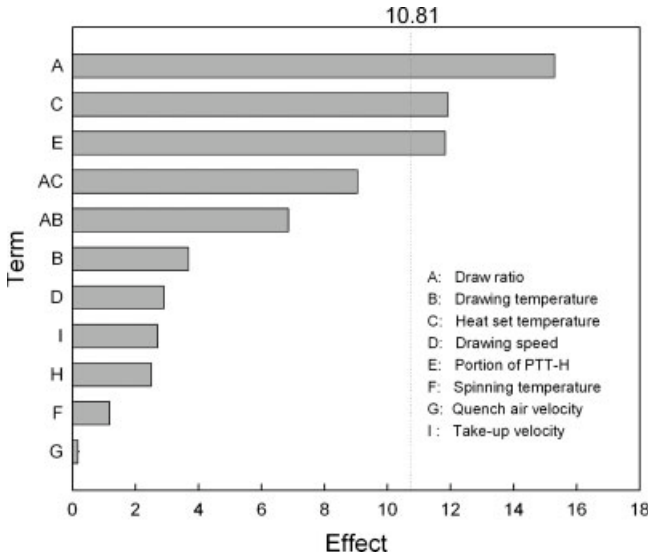

Figure 3 Pareto chart of the screening test.

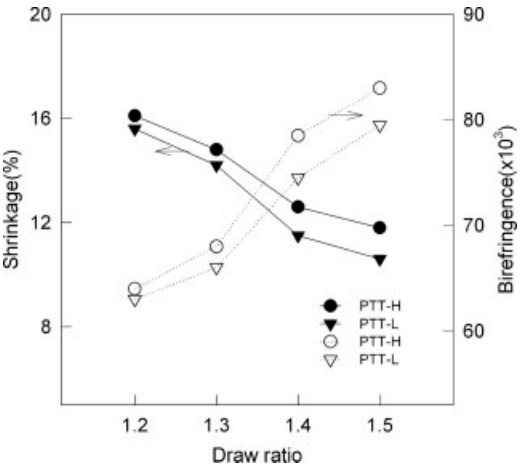

Figure 5 Shrinkage and birefringence of the homofibers of PTT-H and PTT-L as a function of the draw ratio.

draw ratio of 1.4, and this trend can be observed in the shrinkage and birefringence difference of the homofilament (Fig. 5). Figure 5 shows the shrinkage and birefringence of the homofilament spun with only one PTT and under the same process conditions used for the bicomponent fiber. The shrinkage and birefringence difference increase with the draw ratio, and this leads to an increase in the crimp contraction. However, the effect of the draw ratio on the crimp contraction shows a significant change compared with the shrinkage difference of the homofiber. This may be due to stress-induced orientation on the high-viscosity part. In the bicomponent spinning, the molecular orientation of the high-viscosity part increases because of the stress-induced orientation, and that of the low-viscosity part decreases in comparison with homofilament spinning.[19,20] Figure 6 shows the volume fraction crystallinity of the homofilament. The volume fraction crystallinity slightly increases with the draw ratio. The birefringence of fibers is related to the crystallinity and orientation;[21] in general, the crystallinity and orientation increase with increasing draw ratio, and so does the birefringence. However, in the case of the PTT homofilament, the increase in the crystallinity with the draw ratio is not relatively large in the range of draw ratios selected for this experiment. In Chuah's previous work,[22] the crystalline phase orientation of PTT made a small contribution to the birefringence because of the small intrinsic birefringence of the PTT crystal. The birefringence of the PTT crystal was 0.029, which was smaller than that of poly(ethylene terephthalate) (birefringence = 0.22). Also, the crystallinity of the filaments prepared at a velocity range lower than 4 km/min was lower than 25%, and the crystallinity increased gently with the take-up speed.[23] Thus, the crystallinity of the fibers spun at less than 4 km/min made a smaller contribution to the birefringence; the amorphous orientation contribution to the birefringence was dominant. In this experiment, the final converted take-up speeds (take-up speed × draw ratio) were lower than 4 km/min. As shown in Figures 5 and 6, it can be inferred that the crimp contraction of the bicomponent PTT fiber is mainly affected by the amorphous orientation because the oriented amorphous molecule shrinks easily after a boiling-water treatment. The amorphous orientation was dominant in the ranges of the take-up speed and draw ratio of this experiment, like the previous work.[22,23]

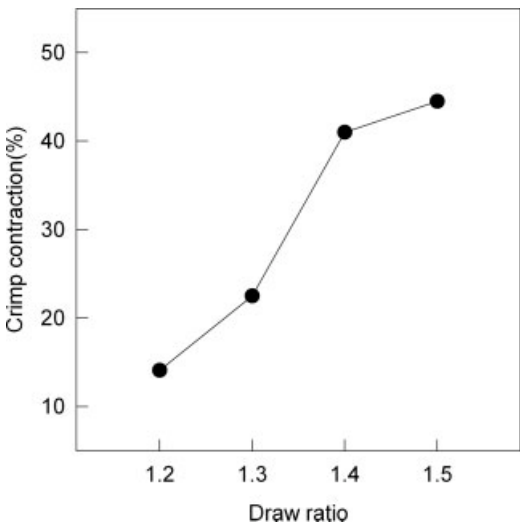

Figure 4 Crimp contraction as a function of the draw ratio.

Effect of the heat-set temperature

Figure 7 shows the effect of the heat-set temperature on the crimp contraction. The crimp contraction increases with the heat-set temperature. The change in the heat-set temperature is not accompanied by a

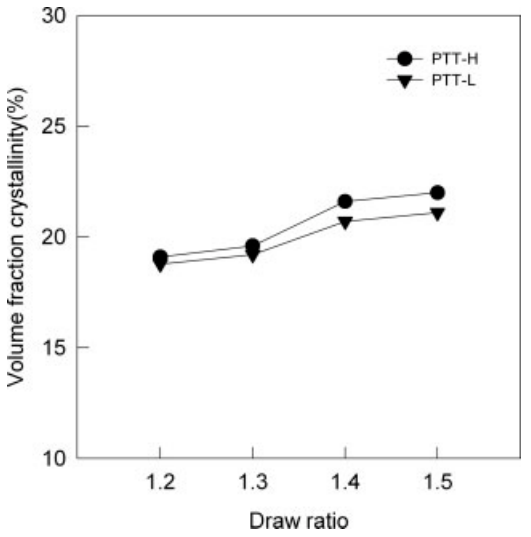

Figure 6 Volume fraction crystallinity of the homofibers of PTT-H and PTT-L as a function of the draw ratio.

dimensional change at a fixed draw ratio. Although there is no a longitudinal dimensional change with the heat-set temperature, the change in the crimp contraction is significant; the extension of the molecular chain is the same at a fixed draw ratio, but the crimp contraction varies with the heat-set temperature. Figure 8 is a plot of the shrinkage of the homofilament. The shrinkage decreases with the heat-set temperature, and the shrinkage difference slightly increases; the increased shrinkage difference induces an increase in the crimp contraction at a higher heat-set temperature. However, the increase in the shrinkage difference is not as large as that of the crimp contraction. This may be due to the difference in the relaxation of the molecular orientation with the heat-set temperature. As the heat-set temperature increases, the crystal structure is stabilized, and the relaxation of the amorphous oriented molecules is restricted. Thus, the amorphous orientation of the high-viscosity part is well maintained at a higher heat-set temperature; this leads to an increased shrinkage difference. Crystallinity usually increases with the heat-set temperature, but it needs enough residence time at a certain annealing temperature.[24–26] In this experiment, the residence time of the filaments in a noncontact-type heat plate in the drawing machine was 0.043 s, and this was not enough time to increase the crystallinity of the drawn fibers.[27] However, as the heat-set temperature increases, the relaxation of the more oriented amorphous region of the PTT-H part is retarded, and the shrinkage difference of the two parts after boiling becomes greater with the heat-set temperature.

Effect of the portion of PTT-H

Like the heat-set temperature, the change in the portion of the high-viscosity polymer affects the crimp contraction with a dimensional change. The crimp contraction increases with the portion of PTT-H (Fig. 9). According to Fitzgerald and Knudsen's theoretical study, the crimp potential is at a maximum when the interface passes through the center of the fiber cross section; that is, when the portion of each part is equal, the crimp contraction is at its maximum.[6] However, the theory is not applicable to this experiment. If the portion of PTT-H increases, the residence time of the PTT-H part decreases in the molten state, and this leads to a decrease in the thermal degradation of PTT. On the contrary, the residence time of PTT-L increases, and this promotes the thermal degradation of PTT-L. The residence

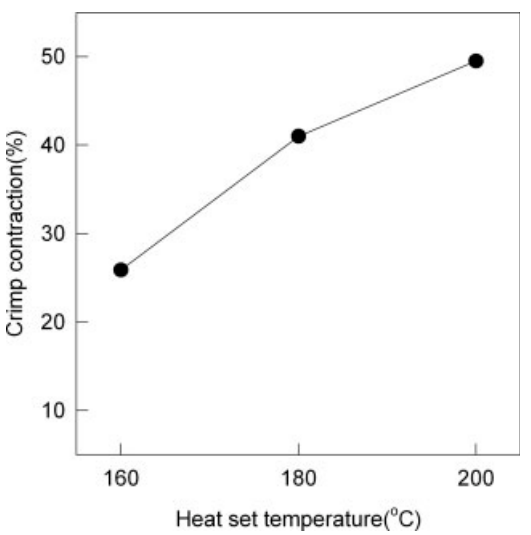

Figure 7 Crimp contraction as a function of the heat-set temperature.

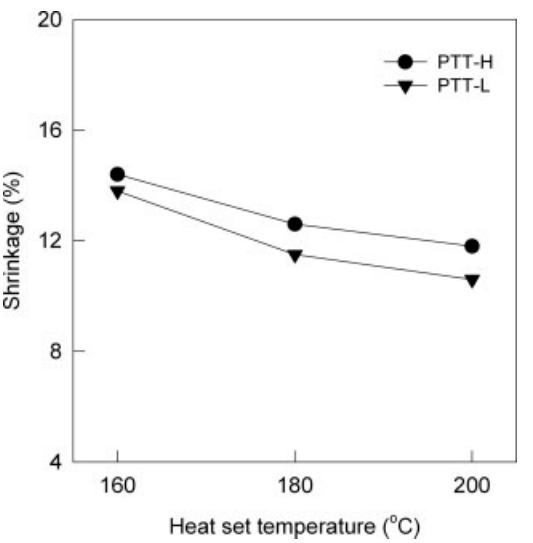

Figure 8 Shrinkage of the homofibers of PTT-H and PTT-L as a function of the heat-set temperature.

time means the measured time that is required for the molten polymer to be spun from the extruder to the spinneret. Figure 10 shows the residence times and IVs of PTT-H and PTT-L. The IV of PTT decreases with increasing residence time, and the IV difference between the two polymers increases with the portion of PTT-H. The molecular chain length difference increases with the high-viscosity portion, and this leads to an increase in the crimp contraction of the fiber after drawing. However, the spinning performance is not good with more than 65% PTT-H. When side-by-side bicomponent fibers composed of polymers of two different viscosities are spun, the extrudate becomes bent toward the direction of the high-viscosity polymer.[28] Large viscosity differences that result from a small amount of PTT-L could affect the spinnability of the fiber because the magnitude of the extrudate exit angle increases with the portion of PTT-H. The increased extrudate exit angle results in poor spinnability.

CONCLUSIONS

The effects of process conditions on crimp contraction in the side-by-side bicomponent spinning and drawing of two PTTs of different viscosities were studied. PTTs with IVs of 1.02 and 0.92 were selected to make a latent crimp yarn. The draw ratio, heat-set temperature, and portion of PTT-H were the main effective process variables. An analysis of the effect of spinning and drawing conditions on the crimp contraction showed that the draw ratio was the most critical variable in controlling it. Increasing the draw ratio caused a difference in the shrinkage between the two parts of PTT and caused self-crimping of the fibers. The obtainable maximum crimp contraction was about 50% at a draw ratio of 1.4 and a heat-set temperature of 200°C. Although there was no dimensional change with the heat-set temperature and portion of PTT-H, they had an influence on the crimp contraction. As the heat-set temperature and portion of PTT-H increased, the crimp contraction of the latent crimp yarn also increased.

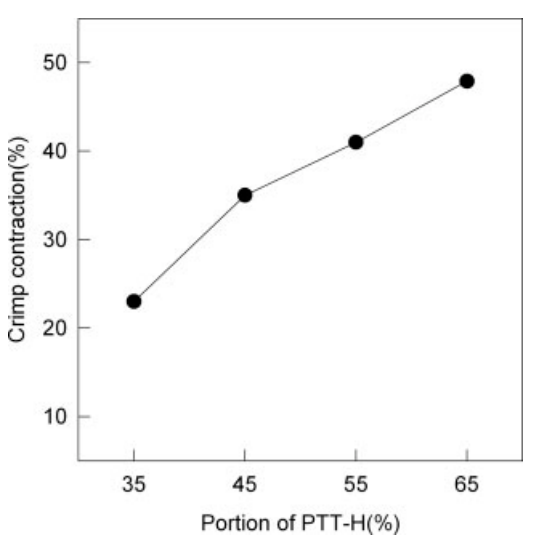

Figure 9 Crimp contraction as a function of the portion of PTT-H.

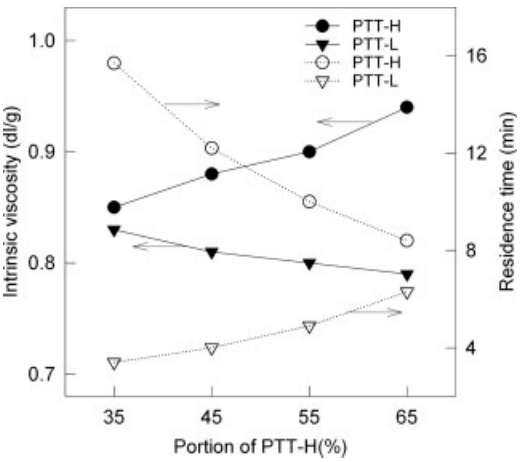

Figure 10 IVs and residence times of PTT-H and PTT-L.

References

1. Washino, Y. Functional Fibers; Toray Research Center: Tokyo, 1993.
2. Bhuvanesh, Y. C.; Gupta, V. B. J Appl Polym Sci 1991, 58, 663.
3. Hongu, T.; Phillips, G. New Fibers; Ellis Horwood: New York, 1990.
4. Matsui, M. Sen-I Kikai Gakkaishi 1981, 34, 319.
5. Matsumoto, T. K. Text Res J 1981, 51, 18.
6. Jeffries, R. Bicomponent Fibers; Marrow: Manchester, UK, 1971.
7. Timoshenko, S. S. J Opt Soc Am 1925, 11, 233.
8. Brown, T. D.; Onions, W. J. J Text Inst 1961, 52, 101.
9. Brand, R. H.; Becker, S. Text Res J 1962, 32, 39.
10. Gupta, B. S.; George, T. W. Text Res J 1975, 45, 338.
11. Fitzgerald, W. E.; Knudsen, J. P. Text Res J 1967, 37, 447.
12. Dangseeyun, N.; Srimoaon, P.; Supaphol, P.; Nithitanakul, M. Thermochim Acta 2004, 409, 63.
13. Chuah, H. H. Macromolecules 2001, 34, 6985.
14. Grebowicz, J. S.; Brown, H.; Chuah, H.; Wasiak, A.; Sajkiewicz, P.; Ziabicki, A. Polymer 2001, 42, 7153.
15. Wu, J.; Schultz, J. M.; Samon, J. M.; Pangelinan, A. B.; Chuah, H. H. Polymer 2001, 42, 7141.
16. Wu, Y.; Wu, A. Taguchi Methods for Robust Design; McGraw-Hill: New York, 2000.
17. Daubeny, R. P.; Bunn, C. W.; Brown, C. J. Proc R Soc London Ser A 1954, 226, 531.
18. Desborough, I. J. Polymer 1979, 20, 545.
19. Radhakrishnan, J.; Kikutani, T. Text Res J 1997, 67, 684.
20. Radhakrishnan, J.; Kikutani, T. Polym Eng Sci 1999, 39, 89.
21. Stein, R. S.; Norris, F. H. J Polym Sci 1956, 21, 381.
22. Chuah, H. H. J Appl Polym Sci 2002, 40, 1513.
23. Wu, G.; Li, H.; Wu, Y.; Cuculo, J. A. Polymer 2002, 43, 2002.
24. Gupta, V. B.; Ramesh, C.; Gupta, A. K. J Appl Polym Sci 1984, 29, 4203.
25. Vasanthan, N. Text Res J 2004, 74, 545.
26. Qureshi, N.; Stepanov, E. V.; Schiraldi, D.; Hilter, A.; Baer, E. J Polym Sci Part B: Polym Phys 2000, 38, 1679.
27. Rao, I. J.; Rajagopal, K. R. Polym Eng Sci 2004, 44, 123.
28. Han, C. D. J Appl Polym Sci 1975, 19, 1875.